Molecular Cell
Article

AKAP-Lbc Mobilizes a Cardiac Hypertrophy Signaling Pathway

Graeme K. Carnegie,[1,6] Joseph Soughayer,[1,6] F. Donelson Smith,[1] Benjamin S. Pedroja,[1] Fang Zhang,[1] Dario Diviani,[2] Michael R. Bristow,[3] Maya T. Kunkel,[4] Alexandra C. Newton,[4] Lorene K. Langeberg,[1] and John D. Scott[1,5,*]
[1]Howard Hughes Medical Institute, Vollum Institute, Oregon Health and Science University, Portland, OR 97239, USA
[2]Pharmacology and Toxicology Department, University of Lausanne CH-1005, Lausanne, Switzerland
[3]Division of Cardiology, University of Colorado Health Sciences Center, Denver, CO 80262, USA
[4]Department of Pharmacology, University of California San Diego, La Jolla, CA 92093, USA
[5]Present address: Howard Hughes Medical Institute, Department of Pharmacology, University of Washington School of Medicine, Seattle, WA 98195, USA
[6]These authors contributed equally to this work
*Correspondence: scottjdw@u.washington.edu
DOI 10.1016/j.molcel.2008.08.030

SUMMARY

Elevated catecholamines in the heart evoke transcriptional activation of the Myocyte Enhancer Factor (MEF) pathway to induce a cellular response known as pathological myocardial hypertrophy. We have discovered that the A-Kinase Anchoring Protein (AKAP)-Lbc is upregulated in hypertrophic cardiomyocytes. It coordinates activation and movement of signaling proteins that initiate MEF2-mediated transcriptional reprogramming events. Live-cell imaging, fluorescent kinase activity reporters, and RNA interference techniques show that AKAP-Lbc couples activation of protein kinase D (PKD) with the phosphorylation-dependent nuclear export of the class II histone deacetylase HDAC5. These studies uncover a role for AKAP-Lbc in which increased expression of the anchoring protein selectively amplifies a signaling pathway that drives cardiac myocytes toward a pathophysiological outcome.

INTRODUCTION

Heart disease is a complex disorder that is a leading cause of death worldwide. Unfavorable environmental factors and genetic profiles contribute to the etiology of several cardiac disorders. These factors can adversely modify heart muscle contraction by interfering with the fine-tuning of cardiomyocyte signal transduction cascades (Bassel-Duby and Olson, 2006). Activation of β-adrenergic receptors during periods of cardiac stress initially improves cardiac output by increasing heart rate and contractility. However, chronic mobilization of the same signaling pathway ultimately harms the heart (Perrino and Rockman, 2007). This is compounded by increased risk factors such as arterial hypertension and valvular heart diseases that place additional biomechanical stress on the heart, inducing a cellular response known as pathological cardiac hypertrophy. Hallmarks of this syndrome include increased cardiomyocyte size and a greater organization of the sarcomere (Frey and Olson, 2003). At the molecular level, hypertrophic signals, such as elevated adrenergic activity, evoke transcriptional activation of the Myocyte Enhancer Factor (MEF) (Bassel-Duby and Olson, 2006). This induces a reprogramming of cardiac gene expression that drives cardiomyocytes toward a development paradigm known as the "fetal gene response" (Molkentin and Dorn, 2001).

A body of work suggests that signaling from the plasma membrane to the transcription factor MEF2 is altered during pathological cardiac hypertrophy (Black and Olson, 1998). MEF2 activity is controlled through its direct association with histone deacetylases (HDACs). These enzymes deacetylate nucleosomal histones, thus promoting chromatin condensation and transcriptional repression (Kouzarides, 2007). The class II histone deacetylases (HDACs 4, 5, 7, and 9) are preferentially expressed in muscle cells (Grozinger and Schreiber, 2000). Phosphorylation of these enzymes by calmodulin dependent (CaM) kinases or the related protein kinase D releases them from association with MEF2 to permit their export from the nucleus (Backs et al., 2006; Bers and Guo, 2005; Sucharov et al., 2006; Vega et al., 2004; Wu et al., 2006). The ensuing derepression of MEF2 activity favors transcription of cardiac genes that promote the fetal gene response causing a hypertrophic phenotype (Chang et al., 2005). Although each component in this pathway is well defined, much less is known about their integration into a dynamic cell-signaling cascade.

Cardiac A-Kinase Anchoring Proteins (AKAPs) play an active role in this process by incorporating protein kinases, protein phosphatases, guanine nucleotide exchange factors, and phosphodiesterases (PDEs) into signaling complexes that respond to catecholamine-evoked changes in the production of second messengers (Chen et al., 2007; Dodge-Kafka et al., 2005; Fink et al., 2001; Lygren et al., 2007). In cardiomyocytes, AKAP-Lbc functions as a scaffolding protein for PKA and PKC to mediate activation of a third enzyme, protein kinase D (PKD1) (Carnegie et al., 2004). In this report, we show that AKAP-Lbc is upregulated in response to hypertrophic stimuli and functions to enhance the efficiency of signaling through a PKD/HDAC5/MEF2 pathway that elicits the fetal gene response.

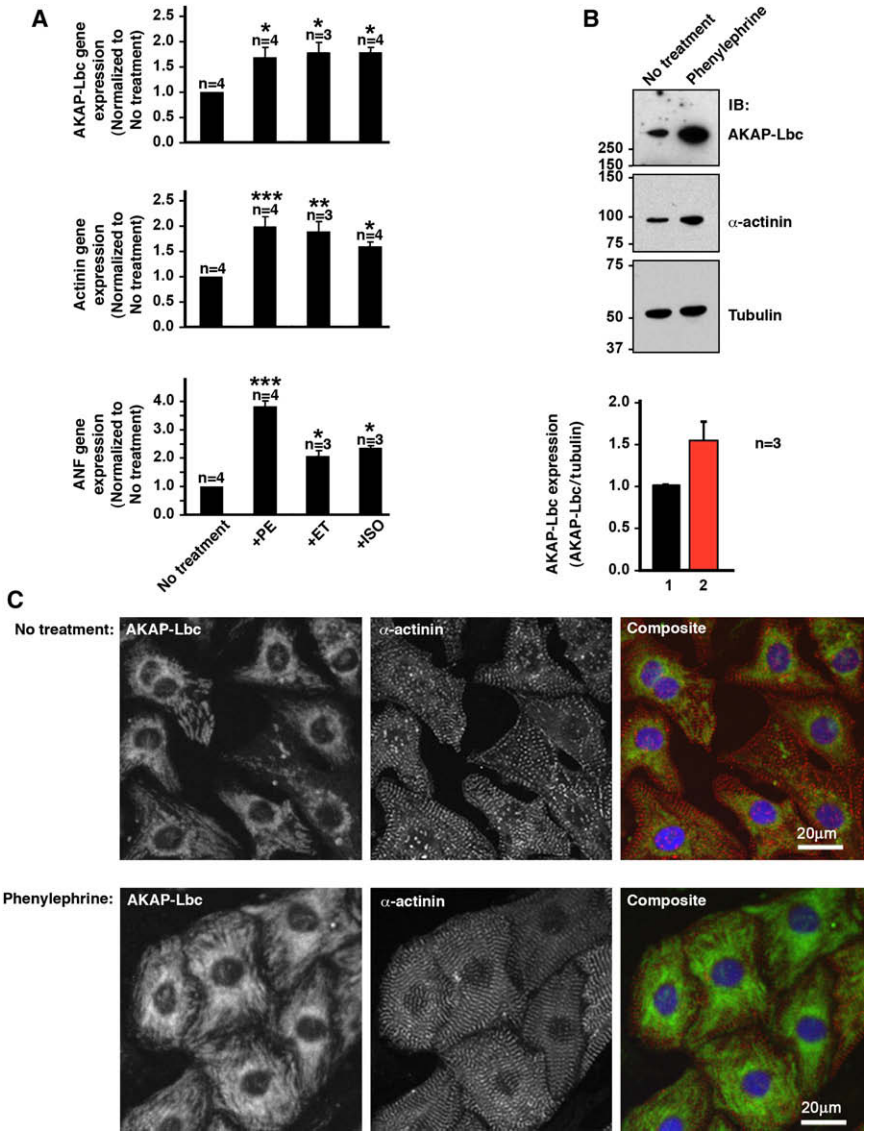

Figure 1. AKAP-Lbc Expression Is Elevated in Hypertrophic Rat Neonatal Cardiomyocytes

(A) RT-PCR analysis of gene expression from RNA prepared from rat neonatal cardiomyocytes (NRVM) treated with hypertrophic agonists. Cells were treated with agonists for 48 hr prior to lysis with TriZol and preparation of RNA. All gene expression data were normalized to GAPDH gene expression. AKAP-Lbc (top panel), α-actinin (middle panel), and ANF (bottom panel). Lane 1: no treatment; lane 2: PE, phenylephrine (working concentration, 10 μM); lane 3: ET, endothelin-1 (working concentration: 100 nM); lane 4: ISO; isoproterenol (working concentration: 10 μM).

Data are expressed as mean ± SEM. Differences in quantitative variables were examined by one-way analysis of variance (ANOVA). A p value < 0.05 was considered significant (*), a p value < 0.01 was considered very significant (**), and a p value < 0.001 was considered extremely significant (***). All analyses were performed using InStat.

(B) Immunoblot detection of AKAP-Lbc (top), α-actinin (middle), and tubulin (bottom) in control and PE-treated NRVM. Cells were treated with PE for 48 hr prior to lysis. Quantitation of the average amounts of AKAP-Lbc was performed over three independent experiments. Data are expressed as mean ± SEM. NIH ImageJ software was used to calculate the relative intensity of each AKAP-Lbc signal normalized to a tubulin loading control.

(C) Immunocytochemical detection of AKAP-Lbc in control and PE-treated NRVM. Cells were treated with PE for 48 hr prior to fixation, permeabilization, and immunostaining. Immunodetection of AKAP-Lbc (green, left panels), immunostaining for the sarcomeric marker protein α-actinin (red, middle panels), and composite images with the nuclear stain DAPI (blue, right panels) are presented. Images were collected on a BioRad MRC 1024 confocal microscope using identical settings for control and hypertrophic NRVM.

RESULTS

AKAP-Lbc Expression Is Elevated in Hypertrophic NRVM

Initial experiments focused on establishing whether hypertrophic stimuli alter AKAP-Lbc expression. Neonatal rat ventricular myocytes (NRVM) were exposed to the α1 adrenergic agonist phenylephrine (PE, 10 μM) for 48 hr to evoke a cellular model of cardiac hypertrophy (Clerk and Sugden, 1999). Quantitative RT-PCR showed that PE induced AKAP-Lbc mRNA levels 1.7 ± 0.2 fold (n = 4) over untreated cells (Figure 1A, top panel, column 2). Data were normalized against the glyceraldehyde-3-phosphate dehydrogenase (GAPDH) gene. Comparable increases in AKAP-Lbc mRNA levels were measured in NRVM treated with other hypertrophic agents, such as endothelin (ET, 100 nM) (1.8 ± 0.2, n = 3) and isoproterenol (ISO, 10 μM) (1.8 ± 0.1, n = 4) (Figure 1A, top panel, columns 3 and 4). Control experiments confirmed that each agonist upregulated two hypertrophic marker genes, atrial natriuretic factor (ANF) and α-actinin (Figure 1A, middle and bottom panels, columns 2–4).

Parallel studies monitored changes in AKAP-Lbc protein levels following PE treatment of NRVM (Figure 1B). AKAP-Lbc was elevated 1.5 ± 0.2-fold (n = 3) over untreated controls. (Figure 1B, top panel, lane 2). Increased expression of α-actinin indicated hypertrophy (Figure 1B, middle panel, lane 2) and tubulin immunoblotting demonstrated equivalent protein loading (Figure 1B, bottom panel). Cellular changes in AKAP-Lbc were further evaluated by immunocytochemistry. Affinity-purified antibodies were used to detect the anchoring protein (green) in control NRVM (Figure 1C). Cells were also stained with the sarcomeric marker α-actinin (red) and DAPI (blue) to denote the nucleus (Figure 1C, top panels). PE treatment increased cell size and enhanced the AKAP-Lbc staining concentrated in perinuclear regions when compared to untreated NRVM (Figure 1C). Taken together, these data illustrate that AKAP-Lbc is elevated in hypertrophic cardiomyocytes. These results substantiate gene array data showing

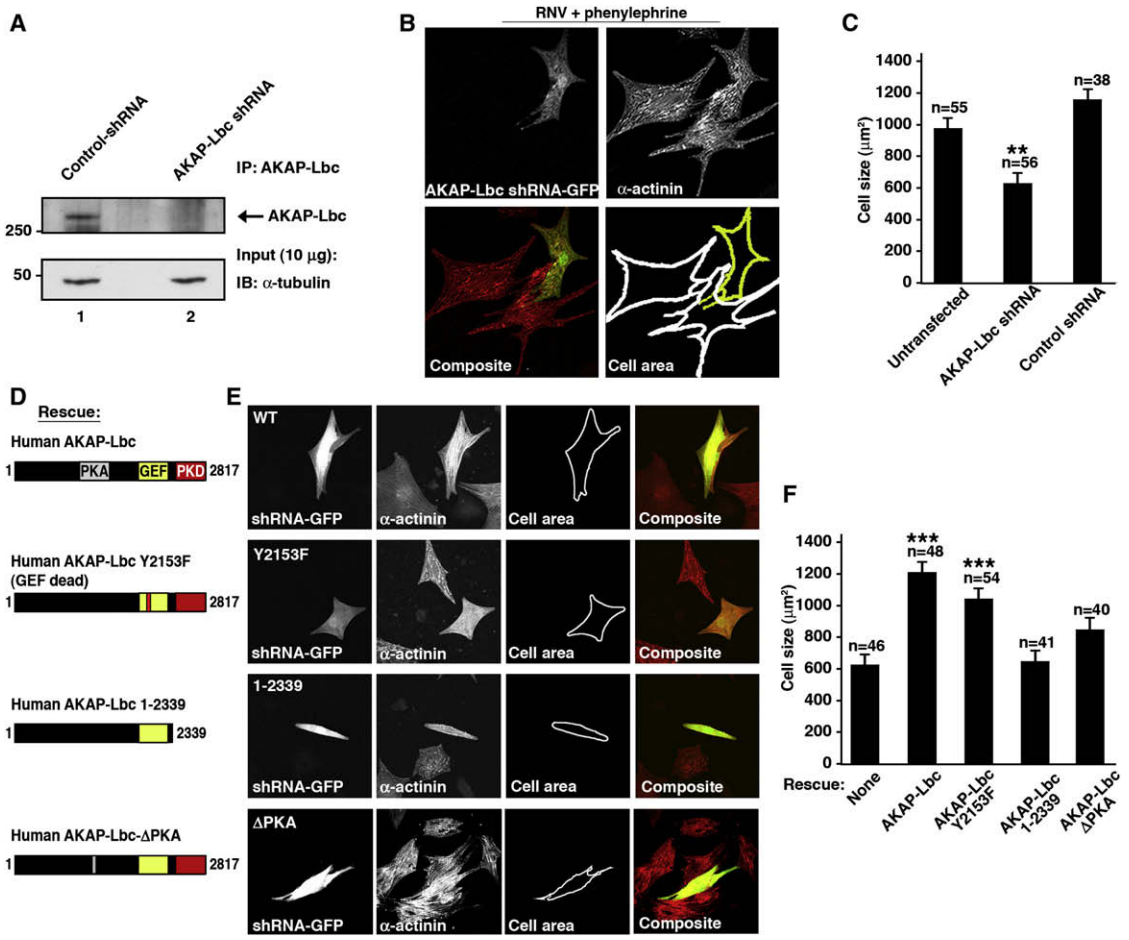

Figure 2. Effects of RNAi Knockdown of AKAP-Lbc in NRVM

(A) Immunoblot showing RNAi knockdown of AKAP-Lbc in NRVM. Endogenous AKAP-Lbc was immunoprecipitated from NRVM lysates after 72 hr exposure to shRNA. Proteins were separated by SDS-PAGE and detected by western blot. AKAP-Lbc, top panel; tubulin loading control, lower panel.

(B) Detection of AKAP-Lbc shRNA/GFP and measurement of cell size in hypertrophic NRVM. NRVM expressing AKAP-Lbc shRNA/GFP were detected by green fluorescence (top left panel). NRVM were fixed and stained for α-actinin (red, top right panel) 72 hr after transfection of shRNA and incubation with PE (for 48 hr). A composite image is presented (bottom, left panel). The outlines for control NRVM (white) and cells infected with the AKAP-Lbc shRNA-GFP (yellow) are indicated (bottom, right panel).

(C) The cell size of untransfected NRVM, cells expressing AKAP-Lbc shRNA/GFP, or a control shRNA was measured using NIH Image J software. NRVM were treated with PE for 48 hr prior to analysis. The amalgamated data are presented (number of cells measured in each group is indicated). All data are expressed as mean ± SEM. Differences in quantitative variables were examined by one-way analysis of variance (ANOVA). A p value < 0.05 was considered significant (*), a p value < 0.01 was considered very significant (**), and a p value < 0.001 was considered extremely significant (***). All analyses were performed using InStat.

(D) Schematic diagram of human AKAP-Lbc constructs used to rescue the anchoring protein shRNA phenotype: hAKAP-Lbc, hAKAP-Lbc-Y2153F (a GEF-dead mutant), hAKAP-Lbc-ΔPKA (a mutant unable to bind PKA), and AKAP-Lbc 1-2339 (a C-terminal truncation mutant that is unable to bind PKD; Figure S3).

(E) Measurement of cell size in hypertrophic cells expressing AKAP-Lbc shRNA/GFP with human AKAP-Lbc rescue constructs. NRVM were fixed and stained for α-actinin (red) 72 hr after transfection of shRNA and incubation with PE. NRVM expressing AKAP-Lbc shRNA/GFP were detected by green fluorescence. Coexpression of rescue constructs was verified by anti-FLAG immunostaining (Figure S2C).

(F) Measurement of cell size following PE treatment. Control NRVM (column 1), NRVM expressing hAKAP-Lbc (column 2), hAKAP-Lbc-Y2153F (column 3), AKAP-Lbc 1-2339 (column 4), and AKAP-Lbc-ΔPKA (column 5). All data are expressed as mean ± SEM. Differences in quantitative variables were examined by one-way analysis of variance (ANOVA). A p value < 0.05 was considered significant (*), a p value < 0.01 was considered very significant (**), and a p value < 0.001 was considered extremely significant (***). All analyses were performed using InStat.

that this anchoring protein (also called AKAP13) is elevated in the hearts of mice with heart failure (van Oort et al., 2006).

Gene Silencing of AKAP-Lbc in NRVM

RNA interference (RNAi) was used to test whether reduced expression of the anchoring protein perturbed aspects of the hypertrophic response. Lentiviral vectors were used to maximize the infection of NRVM with shRNA-GFP constructs (Appert-Collin et al., 2007). Gene silencing was confirmed upon immunoblot analysis of AKAP-Lbc immune complexes (Figure 2A, top panel, lane 2). Detection of tubulin was used as a loading control (Figure 2A, bottom panel). Cells expressing the AKAP-Lbc shRNA

constructs were identified by GFP fluorescence (Figure 2B, top left panel). Immunostaining for α-actinin identified all NRVM (Figure 2B, top right panel). A composite image is presented (Figure 2B, bottom left panel). Phenylephrine effects were assessed by two independent methods: measuring changes in cell size (Kodama et al., 2000) (Figure 2B, bottom right panel) and immunocytochemical detection of ANF (Figure S1). Following treatment with PE, the cells transfected with control shRNA were 1.8 ± 0.2-fold larger (n = 38) than NRVM expressing the rat AKAP-Lbc-shRNA/GFP construct (Figure 2C, columns 2 and 3). Likewise, significant ANF expression was induced by PE treatment of control shRNA cells, whereas induction of ANF was barely detected in cells expressing the AKAP-Lbc shRNA construct (Figure S1). Thus, gene silencing of AKAP-Lbc blunts PE-induced hypertrophic responses in NRVM.

Additional support for this notion was provided by experiments that combined RNAi silencing of the endogenous anchoring protein and rescue with human AKAP-Lbc forms that are refractory to the rat-specific shRNA (Figures 2D–2F). Rescue with full-length human AKAP-Lbc ortholog induced a 1.9 ± 0.1-fold increase (n = 48) in average cell size compared to NRVM where the endogenous rat anchoring protein was knocked down (Figures 2D–2F). AKAP-Lbc is a chimeric molecule that functions as a kinase-anchoring protein and a guanine nucleotide exchange factor (GEF) for the small molecular weight GTPase Rho (Diviani et al., 2001). Both enzyme classes have been implicated in the onset of cardiac hypertrophy (Clerk and Sugden, 2000). Therefore, gene silencing/rescue experiments were performed with modified AKAP-Lbc forms to delineate the contribution of each signaling pathway in the PE response. When NRVM were rescued with the AKAP-Lbc Y2153F mutant that lacks Rho GEF activity, we observed an agonist-induced increase in cell size (1.7 ± 0.1 fold, n = 54, Figures 2D–2F) and elevated ANF levels (Figure S2). A smaller agonist-induced increase in cell size (1.2 ± 0.2 fold, n = 40, Figures 2D–2F) was observed when NRVM were rescued with the AKAP-Lbc-ΔPKA mutant that cannot anchor PKA. Thus, anchoring of PKA may also contribute to this process. However, a more significant observation was that phenylephrine induced increases in NRVM size and ANF expression was blocked when rescue experiments were performed with a truncated AKAP-Lbc form (AKAP-Lbc 1–2339) that does not bind PKD1 (Figures 2D–2F and Figures S2 and S3). These latter results imply that the PKD scaffolding function of AKAP-Lbc is the principle factor in transduction of the hypertrophic response. Additional mapping experiments identified multiple PKD1-binding sites in the C-terminal quarter of AKAP-Lbc (Figure S4).

AKAP-Lbc Facilitates Nuclear Export of HDAC5

A variety of kinase signaling pathways induce cardiac gene reprogramming during hypertrophy. A major pathway involves phosphorylation of class II HDACs (HDACs 4, 5, 7, and 9) by the calmodulin-dependent kinases CaMKII or CaMKIV, or by PKD (McKinsey, 2007). Phosphorylation of HDACs promotes their nuclear export, resulting in derepression of MEF2 activity and concomitant activation of target genes to propagate the hypertrophic response (Figure 3A). Recent investigations suggest that CaM kinases selectively target HDAC4, whereas PKD1 preferentially regulates HDAC5 action (Backs et al., 2006; Wu et al., 2006). Therefore, we postulated that AKAP-Lbc may facilitate the activation of the PKD1 isoform to enhance nuclear export of HDAC5.

Initial support for this model was provided by live-cell imaging experiments in Cos7 cells. We monitored the movement of fluorescently tagged HDAC5 in response to phorbol ester (PDBu, 50 nM), a pharmacological activator of PKD (Waldron and Rozengurt, 2003). NIH ImageJ software was used to measure the relative intensity of fluorescent signals in defined regions of the nucleus and cytoplasm of each cell. Measurements were conducted at 5 min intervals for the duration of the experiments (Figures 3B–3D). There was no discernable movement of HDAC5-red fluorescent protein (RFP) in control cells for up to 81.3 ± 7 min (n = 36) after the application of PDBu. Yet, the mean time for HDAC5-RFP nuclear export in the presence of AKAP-Lbc-GFP was 42 ± 5 min (n = 41 cells) after the application of PDBu (Figures 3B–3D and Movies S1 and S2). Control experiments were performed with the AKAP-Lbc 1-2339-GFP fragment that is unable to interact with PKD1. The mean time for HDAC5-RFP nuclear export was 67 ± 9 min (n = 32 cells) after the application of PDBu and suggested that AKAP-Lbc influences PKD1 to enhance nuclear export of the histone deacetylase (Figure 3D).

Further studies were performed to assess the contribution of the GEF domain in AKAP-Lbc and CaM kinases in this process. The rate of HDAC5-RFP nuclear export either in the presence of AKAP-Lbc Y2153F (Figure S5) or in cells pretreated with the CaM kinase inhibitor KN93 (Figure S6) was similar to cells expressing AKAP-Lbc-GFP. This suggests that AKAP-Lbc-mediated nuclear export of HDAC5 proceeds via a mechanism that involves activation of PKD1 and that this can occur in a manner that is independent of Rho activation and CaM Kinase activity.

Nuclear export of class II HDACs triggers a fetal gene response in cardiomyocytes through stimulation of a MEF2 transcriptional activation pathway. Therefore, we used a luciferase reporter (provided by Dr. Eric Olson, University of Texas-Southwestern) to examine MEF2-mediated transcription. Cos7 cells express low levels of AKAP-Lbc, PKD, and the histone deacetylase, thereby providing an ideal model cell line to study the role of this pathway in transcriptional activation using the MEF2 reporter. PDBu-dependent stimulation of MEF2 transcription was increased 4.9 ± 1.7-fold (n = 4) in the presence of AKAP-Lbc and was further enhanced to 6.9 ± 1.4-fold (n = 4) upon overexpression of PKD with the anchoring protein (Figure 3E). Controls did not detect any PDBu-dependent stimulation of transcriptional activity driven by a β-galactosidase reporter. These findings strengthen our view that AKAP-Lbc mediated activation of PKD can stimulate MEF2 transcription.

The remainder of our analyses was conducted in primary cultures of NRVM to probe the spatiotemporal dynamics of this signaling pathway in a more appropriate cellular context. Nuclear export of HDAC5-RFP was complete within 66 ± 6 min (n = 12 cells) after application of PDBu in control NRVM (Figure 4A, top panels; Figure 4B, column 1). In cells expressing AKAP-Lbc-YFP, a more rapid PDBu-dependent nuclear export of HDAC5-RFP was observed. Movement of HDAC5 from the nucleus was complete within 33 ± 3 min (n = 21 cells) (Figures 4A and 4B and Movies S3 and S4).

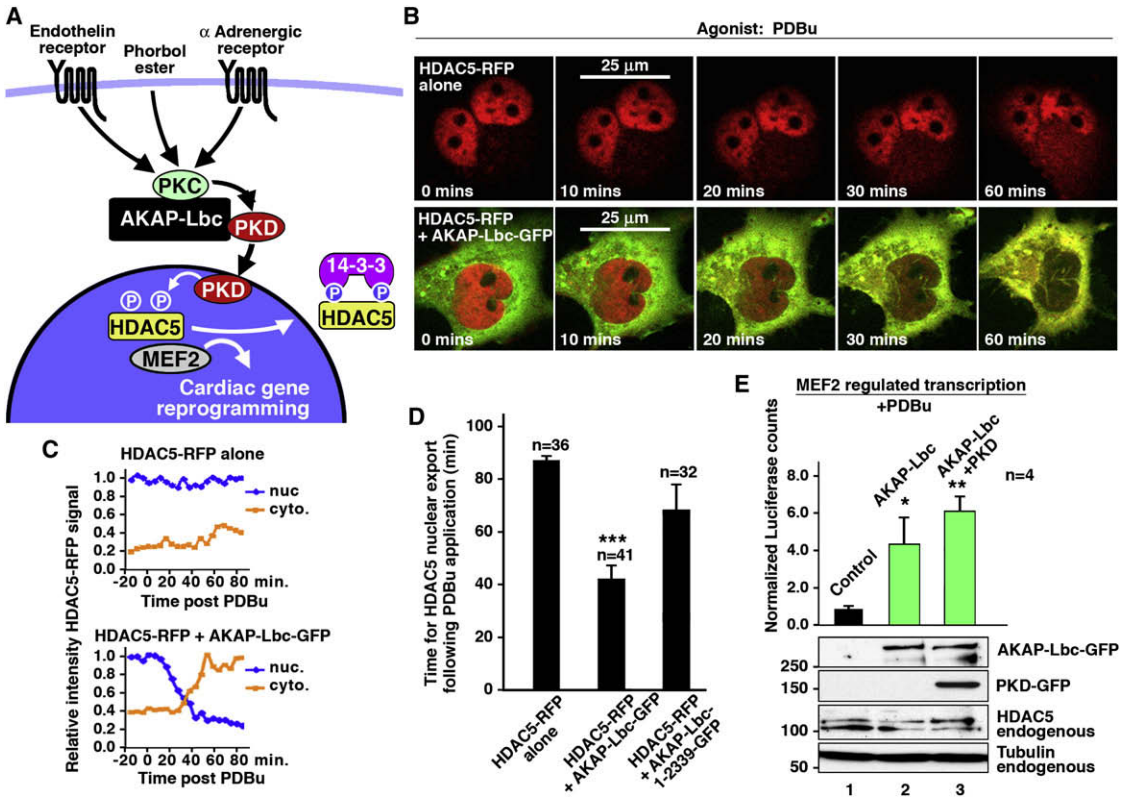

Figure 3. Imaging AKAP-Lbc-Mediated Nuclear Export of HDAC5, and Regulation of Transcription in Cos7 Cells

(A) Schematic diagram depicting the regulation of MEF2 transcription in response to hypertrophic agonists. We postulate that AKAP-Lbc plays a central role in this pathway, facilitating activation of PKD, causing phosphorylation and subsequent nuclear export of HDAC5, thereby leading to derepression of MEF2 transcription and cardiac gene reprogramming events.

(B) Live-cell imaging techniques were used to monitor the cellular location of HDAC5 in Cos7 cells treated with phorbol ester (PDBu). PDBu was applied to Cos7 cells at 0 min, and images were collected at designated times (indicated in each frame). Representative images from cells expressing HDAC5-RFP (red, top panels) and cells coexpressing HDAC5-RFP with AKAP-Lbc-GFP (green, bottom panels).

(C) Quantitation of the relative nuclear and cytoplasmic intensity of HDAC5-RFP signal carried out using NIH Image J software.

(D) Amalgamated data indicating the time of HDAC5 nuclear export in Cos7 cells following application of PDBu. Data are expressed as mean ± SEM. Differences in quantitative variables were examined by ANOVA using the software InStat.

(E) Analysis of MEF2-regulated transcriptional activity in response to PDBu in Cos7 cells coexpressing AKAP-Lbc (lane 2) and PKD + AKAP-Lbc (lane 3). A western blot of lysates shows even loading across samples (tubulin loading control), equal ectopic expression of AKAP-Lbc in lanes 2 and 3, and PKD in lane 4. All data are expressed as mean ± SEM. Differences in quantitative variables were examined by one-way analysis of variance (ANOVA). A p value < 0.05 was considered significant (*), a p value < 0.01 was considered very significant (**), and a p value < 0.001 was considered extremely significant (***). All analyses were performed using InStat.

Similar data were obtained upon stimulation with endothelin-1 (ET-1, 100 nM), a potent vasoconstrictor that is implicated in the onset of myocardial inflammation and hypertrophy (Sugden and Clerk, 2005; Teerlink, 2005). Endothelin-dependent movement of HDAC5-RFP took 53.3 ± 4 min (n = 35 cells) in control cells but was reduced to 34 ± 5 min (n = 21 cells) upon overexpression of the anchoring protein (Figures 4C and 4D and Movies S5 and S6). Finally, we measured the rate of ET-1-dependent HDAC5-RFP nuclear export in cells in which the endogenous rat AKAP-Lbc expression was silenced by RNAi. AKAP-Lbc shRNA and control shRNA cells were identified by the coexpression of GFP as a marker (Figure 4E, first panels). Endothelin-dependent nuclear export of HDAC5-RFP was significantly delayed upon depletion of the anchoring protein [75 ± 5 min, n = 13] as compared to shRNA controls [53 ± 8 min, n = 14] (Figures 4E and 4F and Movies S7 and S8). These data reinforce our contention that AKAP-Lbc contributes to the enhancement of HDAC5 nuclear export in cardiomyocytes.

In Situ Analysis of PKD Activity

Our working hypothesis is that AKAP-Lbc mediated activation of PKD potentiates the hypertrophic response. Accordingly, overexpression of AKAP-Lbc enhanced activation of the kinase as assessed by immunoblot using anti-phospho-PKD Ser 744/748 antibodies when phenylephrine, endothelin, or PDBu was used as the agonist (Figure 5A and Figure S7). The time course of these events was further evaluated using a genetically encoded fluorescence-based D-Kinase Activity Reporter (DKAR) (Kunkel et al., 2007). PKD phosphorylation of a consensus substrate sequence (LSRQLTAAVSE) results in a decrease in Fluorescence

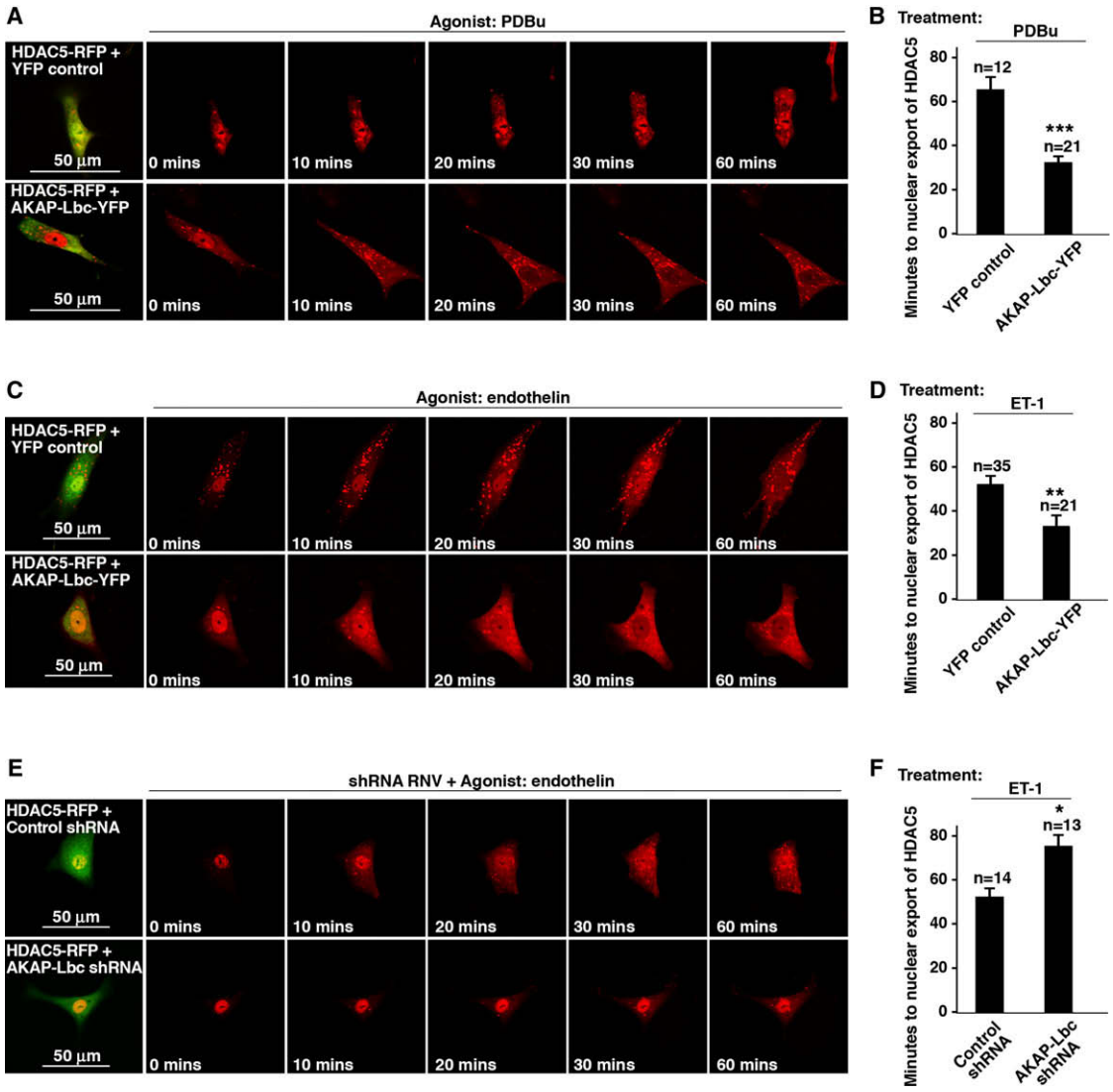

Figure 4. AKAP-Lbc-Mediated HDAC5 Nuclear Export in NRVM

(A) Time course of HDAC5-RFP (red) nuclear export in response to PDBu (top panels), and nuclear export of HDAC5-RFP when coexpressed with AKAP-Lbc-YFP (bottom panels). PDBu was applied to cells at 0 min. AKAP-Lbc-YFP and control cells were identified by YFP fluorescence (first panels).

(B) Amalgamated data indicating the time of HDAC5 nuclear export following application of PDBu in NRVM expressing HDAC5-RFP and YFP (control cells, column 1) or coexpressing HDAC5-RFP with AKAP-Lbc-YFP (column 2). Data are expressed as mean ± SEM. Differences in quantitative variables were examined by ANOVA or an unpaired two-tailed t test. All analyses were performed using InStat.

(C) Time course of HDAC5-RFP (red) nuclear export in NRVM in response to endothelin-1 (ET) (top panels), and nuclear export of HDAC5-RFP when coexpressed with AKAP-Lbc-YFP (bottom panels). ET-1 was applied to cells at 0 min.

(D) Amalgamated data indicating the time of HDAC5 nuclear export following application of ET-1 in NRVM expressing HDAC5-RFP and YFP (control cells, lane 1) or coexpressing HDAC5-RFP with AKAP-Lbc-YFP (column 2). Data are expressed as mean ± SEM. Differences in quantitative variables were examined by ANOVA or an unpaired two-tailed t test using Instat.

(E) The time course of ET-1 nuclear export HDAC5-RFP (red) in NRVM cotransfected with control shRNA (top panels) or NRVM cotransfected with AKAP-Lbc-shRNA (green, bottom panels). ET-1 was applied to cells at 0 min.

(F) Amalgamated data indicating the time of HDAC5 nuclear export following application of ET-1 in NRVM expressing HDAC5-RFP and control shRNA (column 1) or coexpressing HDAC5-RFP with AKAP-Lbc-shRNA (column 2). Data are expressed as mean ± SEM. Differences in quantitative variables were examined by ANOVA or an unpaired two-tailed t test using Instat.

Resonance Energy Transfer (FRET), as measured by dynamic changes in the YFP/CFP ratio (Figure 5B).

A nuclear localization signal (PKKKRKVEDA) was engineered into the parent DKAR construct. This allowed us to selectively monitor PKD activity in the nucleus where HDAC5 is a likely substrate. ET-1 was applied to NRVM at time zero, and fluorescent images were collected at 30 s intervals for 90 min (Figures 5C–5E). Increased PKD activity was scored as a decrease in the

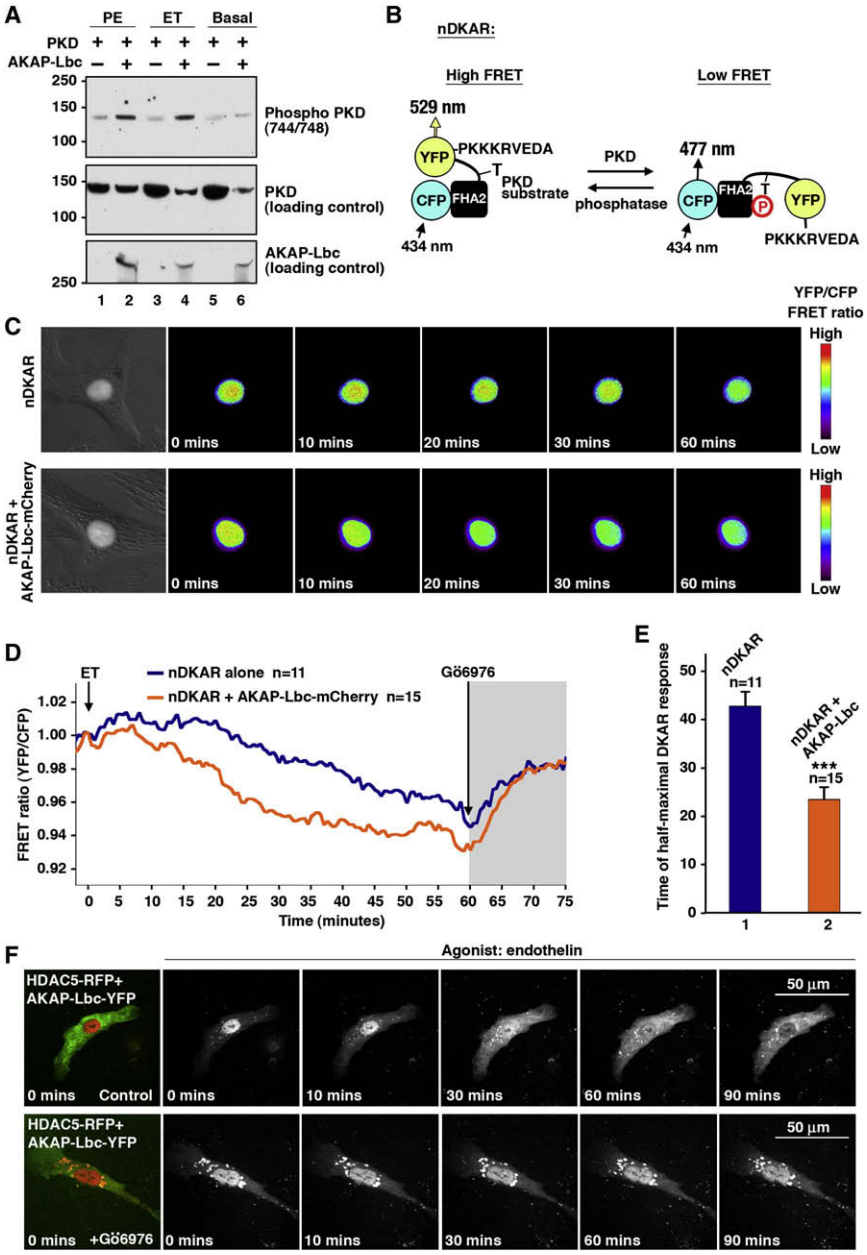

Figure 5. In Situ Analysis of PKD Activity

(A) Activation of PKD by AKAP-Lbc. HEK293 cells expressing PKD alone or coexpressing PKD with AKAP-Lbc were untreated or stimulated with PE or ET-1 prior to lysis. Proteins were separated by SDS-PAGE. PKD activation was assessed by immunoblot using anti-phospho-Ser-744/748 PKD antibodies (top panel). Loading controls for total PKD (middle panel) and AKAP-Lbc (bottom panel) are presented.

(B) Diagram showing the mechanism of action for the nuclear D Kinase Activity Reporter (nDKAR). A decrease in Fluorescence Resonance Energy Transfer (FRET) equates to an increase in PKD activity.

(C) Pseudocolor images following the time-course changes in the nDKAR FRET ratio (YFP/CFP) in NRVM upon stimulation with ET-1. The first panels are brightfield images of the cells, showing the location of nDKAR. Top panels show a typical response of nDKAR after application of ET-1. The bottom panels show a typical response of nDKAR in NRVM coexpressing AKAP-Lbc.

(D) Amalgamated traces of nDKAR FRET ratio in response to ET-1 in NRVM expressing nDKAR alone (blue line, n = 11 cells) or coexpressing nDKAR and AKAP-Lbc (orange line, n = 15 cells). ET-1 was added at 0 min. The selective inhibitor Gö6976 was added after 60 min to block PKD activity.

(E) The time of half-maximal nDKAR response was measured and averaged for cells expressing nDKAR alone (column 1) or cells coexpressing nDKAR and AKAP-Lbc (column 2). Data are expressed as mean ± SEM. Differences in quantitative variables were examined by ANOVA, using the software InStat. A p value < 0.05 was considered significant (*), a p value < 0.01 was considered very significant (**), and a p value < 0.001 was considered extremely significant (***).

(F) Top panels: time course showing nuclear export of HDAC5-RFP when coexpressed with AKAP-Lbc-YFP in NRVM in response to endothelin-1 (ET). Bottom panels: nuclear export of HDAC5-RFP when coexpressed with AKAP-Lbc-YFP in cells treated with the inhibitor Gö6976 prior to ET-1 application (at 0 min).

YFP/CFP ratio in a defined area of the nucleus. Half-maximal responses were reached within 44 ± 3 min (n = 11) following application of ET-1 in NRVM expressing nDKAR alone (Figure 5C, upper panels; Figure 5D, blue line; and Figure 5E, column 1). However, the rate and magnitude of the DKAR response was increased in NRVM expressing AKAP-Lbc-mCherry showing a half maximal activation within 25 ± 3 min (n = 15, Figure 5C, lower panels; Figure 5D, orange line; and Figure 5E, column 2). Control experiments confirmed that the nDKAR FRET ratio was reversed upon application of Gö6976 (500 nM), the most selective, commercially available PKD inhibitor (Figure 5D). Hence AKAP-Lbc acts as a catalyst to favor PKD activation and apparently increases the pool of active enzyme in the nucleus. Both factors drive NRVM toward the nuclear exclusion of HDAC5. Additional imaging experiments confirmed that pretreatment of NRVM with Gö6976 blocks agonist-induced nuclear export of HDAC5-RFP when compared to controls (Figure 5F).

PKA and PKD Catalyze the Phosphorylation-Dependent Recruitment of 14-3-3 and Nuclear Export of HDAC5

A pair of consensus 14-3-3 binding sites have been identified that encompass serine residues 259 and 498 on HDAC5 (McKinsey et al., 2000). Sequence analysis of these regions showed that serine 259 lies within the context of a PKD substrate motif, whereas the amino acid residues surrounding serine 498 form a PKA phosphorylation site. Radiolabeling of HDAC5 with

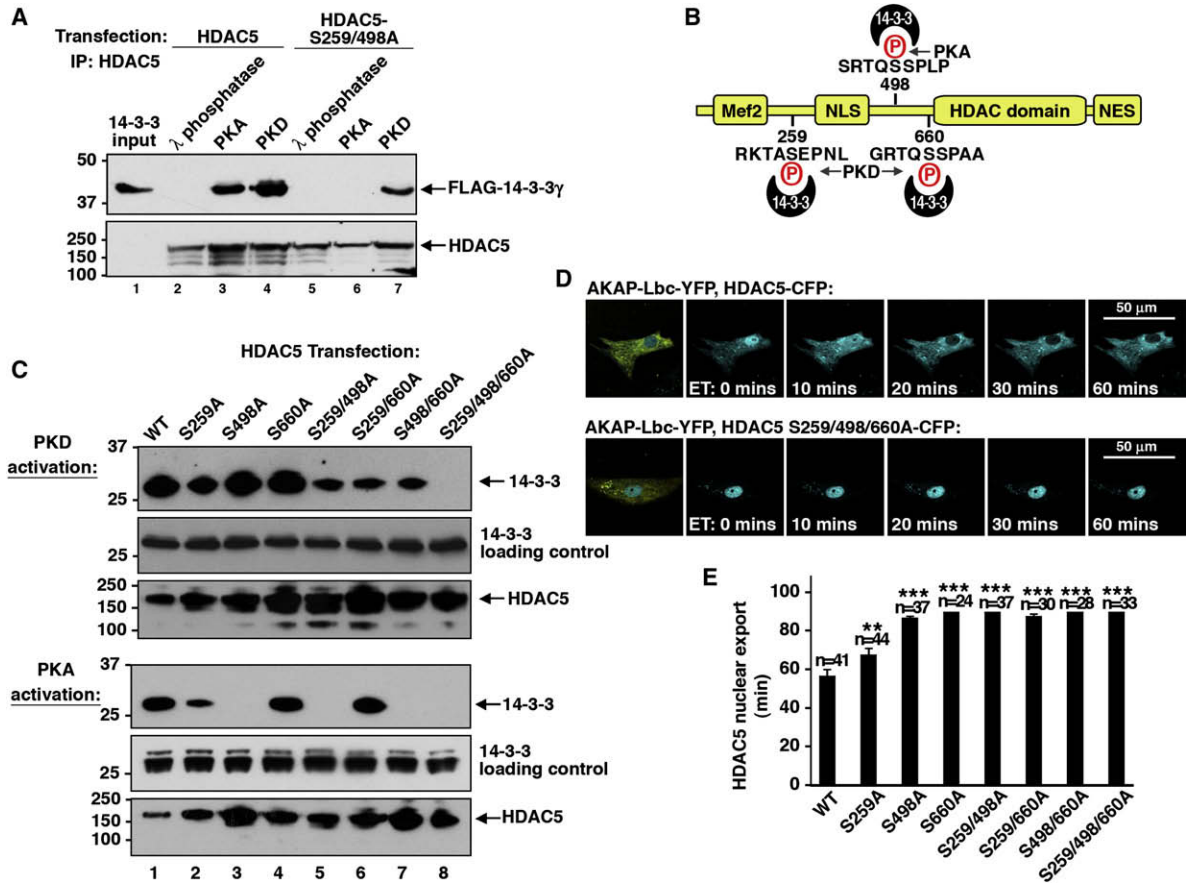

Figure 6. Analysis of HDAC5 Phosphorylation and Induction of 14-3-3-Binding

(A) Phosphorylation of HDAC5 by PKA or PKD induces 14-3-3 binding. Epitope tagged-HDAC5 (lanes 2–4) or an HDAC5-S259/498A double mutant (lanes 5–7) were immunoprecipitated from HEK293 cells and incubated with cell lysates expressing FLAG-14-3-3γ (top panel). 14-3-3 binding was assessed under conditions where HDAC5 was either dephosphorylated by incubation with λ-phosphatase (lanes 2 and 5) or phosphorylated by PKA (lanes 3 and 6) or PKD (lanes 4 and 7) in vitro.

(B) Diagram of phosphorylation sites that regulate 14-3-3 binding on HDAC5. Consensus 14-3-3 binding sites are denoted. Kinase phosphorylation sites are indicated in red.

(C) Mapping the essential 14-3-3 binding sites on HDAC5. A family of seven HDAC5 mutants where serines 259, 498, and 660 were systematically replaced with alanine was screened for interaction with 14-3-3 in HEK293 cells. Experiments were performed using PDBu to activate PKD (top group) or with forskolin/IBMX to activate PKA (bottom group). The presence of 14-3-3 in HDAC5 immune complexes was assessed by immunoblot (top panels). Loading controls for 14-3-3 (middle panels) and HDAC5 (bottom panels) are presented.

(D) Cellular analysis of 14-3-3 binding sites on HDAC5 nuclear export. The movement of each HDAC5 14-3-3 binding mutant was analyzed in NRVM. Representative images of a time course depicting ET-1-dependent response of HDAC-CFP (top panels) and the HDAC5-CFP S259S, S498A, S660A triple mutant (bottom panels).

(E) Graph of amalgamated data from experiments measuring the rate of nuclear export (mins) of each HDAC5 mutant. All data are expressed as mean ± SEM. Statistical significance and number of cells measured is indicated above each column.

purified kinases and peptide array analysis was used to further define the relevant phosphorylation sites on the histone deacetylase (Figure S8). In vitro binding studies confirmed that phosphorylation of HDAC5 by either PKA or PKD1 permitted the recruitment of 14-3-3 (Figure 6A, lanes 1–4). However, 14-3-3 still bound to an HDAC5 S259/498A double mutant upon phosphorylation by PKD1 (Figure 6A, lanes 5–7). This inferred that additional 14-3-3 binding sites must reside on HDAC5. Upon further inspection, another consensus 14-3-3 binding motif was identified that included a possible PKD substrate site at serine 660 (Figure 6B). Cell-based studies with a family of HDAC5 point mutants confirmed this hypothesis (Figure 6C, bottom panel, lane 8). PKD1 dependent recruitment of 14-3-3 was abolished only when all three sites were inactivated by the introduction of a nonphosphorylatable alanine residue (Figure 6C top panel, lane 8). This differed from the PKA dependent recruitment of 14-3-3 that was lost in HDAC5 mutants lacking Ser 498 (Figure 6C, bottom panels, lanes 3, 5, 7, and 8). These observations were consistent with live-cell imaging experiments conducted with CFP tagged versions of the HDAC5. Any HDAC5 point mutant that lacked either Ser 498 or Ser 660 was not exported from the nucleus when compared to the wild-type control (Figure 6D and Movies S9 and S10). In contrast, mutation of serine 259 to alanine minimally reduced the rate of HDAC nuclear export from

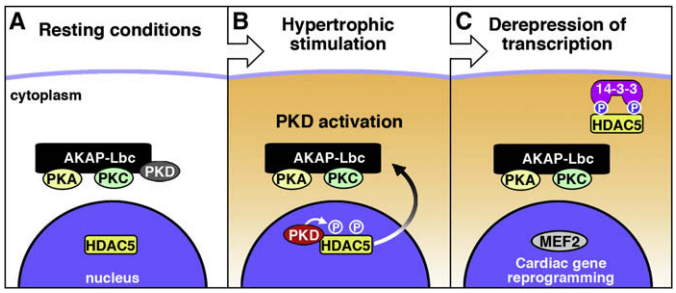

Figure 7. Model Showing the Role of AKAP-Lbc in the Regulation of Cardiac Hypertrophy through the PKD-HDAC5-MEF2 Signaling Pathway
(A–C) See text for details.

57 ± 3 min (n = 41) to 68 ± 3 min (n = 44) when compared to the wild-type control (Figure 6E, column 2). Thus serine residues 498 and 660 may represent the principal phosphorylation sites on HDAC5 that are required for the 14-3-3-dependent nuclear export. Furthermore, two AKAP-Lbc-associated kinases, PKA and PKD1, may cooperate to promote movement of HDAC5 into the cytoplasm.

DISCUSSION

We propose that AKAP-Lbc is a previously unrecognized factor that selectively directs catecholamine signals to the transcriptional machinery to potentiate the hypertrophic response. The anchoring protein is both upregulated under pathophysiological conditions and organizes a signaling pathway that contributes to the onset of myocardial hypertrophy. Although most of our study was conducted in neonatal rat cardiac myocytes, further support for this concept was provided by analysis of human heart tissue samples obtained postmortem from two individuals exhibiting hypertrophic myopathy: a 46-year-old male with a left ventricular ejection fraction (LVEF) of 42% and a 62-year-old female, LVEF 12%. A 2 ± 0.5-fold increase in AKAP-Lbc mRNA was measured over normal age-matched patient controls (Figure S9). While induction of cardiomyopathy is a multifaceted process, we contend that AKAP-Lbc mobilizes a subset of effectors to enhance progression of this syndrome. Our data support a model where AKAP-Lbc facilitates activation of protein kinase D, which in turn phosphorylates the histone deacetylase HDAC5 to promote its nuclear export (Figures 7A and 7B). Finally, the concomitant reduction in nuclear histone deacetylase activity favors MEF2 transcription and the onset of cardiac hypertrophy (Figure 7C).

In response to signals from α_1-adrenergic and endothelin receptors AKAP-Lbc facilitates activation of anchored kinases that mobilize the transcriptional machinery. Signals downstream of the α_1-AR can also stimulate the small molecular weight GTPase Rho during hypertrophy (Maruyama et al., 2002). Additionally, several Rho effectors were identified in a genetic screen for modulators of class II HDAC phosphorylation (Chang et al., 2005). These included Rho-GEF1/p115-GEF, also known as "Lbc's second cousin" (Lsc; mouse ortholog) on the basis of its homology to the anchoring protein. Since AKAP-Lbc also possesses intrinsic Rho guanine nucleotide exchange factor (GEF) activity (Diviani et al., 2001) it was important to delineate whether hypertrophic agonists exert their effects through activation of anchored kinases or via the stimulation of Rho. Two findings point toward kinase scaffolding as the predominant mechanism. First, AKAP-Lbc RNAi/rescue experiments showed that PKD binding is necessary for PE induced hypertrophy, while disruption of the AKAP-Lbc GEF activity had minimal effect (as assessed by cell size or induction of ANF; Figures 2E and 2F and Figure S2). Second, live-cell imaging showed that disruption of the GEF activity in AKAP-Lbc had no effect on the rate of agonist-dependent HDAC5-RFP nuclear export when compared with the wild-type anchoring protein (Figure S5).

While activation of PKD appears to be the primary function of AKAP-Lbc, it should be noted that the anchoring protein may independently contribute to Rho activation through a $G\alpha_{12}$ pathway. It has recently been reported that overexpression of dominant interfering mutants of $G\alpha_{12}$ reduced phenylephrine-induced changes in cardiomyocyte size (Appert-Collin et al., 2007). Therefore AKAP-Lbc may provide a locus for crosstalk between the PKD and Rho signaling pathways in a context-dependent manner. In the immune system, Rho is required for PKD's effects on pre-T cell differentiation at the membrane but is not necessary for PKD activation in the cytoplasm of mature T cells (Mullin et al., 2006). Indeed, AKAP-Lbc may function as a pleiotropic effector by integrating PKD and Rho action in certain subcellular locations while segregating these signaling pathways in other regions of the cell.

Live-cell imaging with FRET-based kinase activity reporters and fluorescently tagged proteins offer different perspectives on the same cellular process. This has enabled us to correlate changes in nuclear PKD activity with HDAC nuclear export. We now have a clearer picture of how individual steps in this hypertrophic signaling pathway are coupled. Overexpression of AKAP-Lbc increases the rate and strength of PKD activation (Figure 5D) and accelerates the nuclear export of HDAC5 (Figures 4A–4D). On the contrary, a reduction in AKAP-Lbc expression (by shRNA) virtually abolishes the movement of the histone deacetylase. Technical limitations precluded the use of DKAR in cells expressing the AKAP-Lbc shRNA with a GFP marker. Regardless, these experiments provide some of the most compelling evidence to date on how AKAPs organize discrete molecular events that relay signals from one cellular compartment to another.

HDACs are primed for nuclear export upon the phosphorylation-dependent recruitment of 14-3-3 proteins (Grozinger and Schreiber, 2000; Kao et al., 2001; McKinsey et al., 2001). Our data add to the understanding of this concept in two ways. First of all, we show that PKA phosphorylation of serine 498 on HDAC5 facilitates 14-3-3 binding. Since PKA and PKD are components of the AKAP-Lbc scaffold, it would appear that HDAC5 phosphorylation may represent a point of convergence for the phospholipid and cAMP signaling pathways. However, PKA phosphorylation alone is not sufficient to induce nuclear export, as treatment with isoproterenol to elevate intracellular cAMP has no effect on HDAC5 translocation in NRVM (data not shown).

Second, we have characterized an additional and physiologically relevant 14-3-3 interaction site at serine 660 of the histone

deacetylase. This site acts in conjunction with the previously recognized sites at serines 259 and 498. Phosphorylation of two of these sites is required for nuclear export as mutation of either Serine 498 or Serine 660 blocks HDAC5 movement. In contrast, mutation of Ser 259 reduces 14-3-3 binding but has a negligible effect on HDAC5 movement (Figures 6B and 6E). These observations tally with current models for 14-3-3 action where the dimeric protein sequentially binds a pair of phosphoserine motifs on its binding partner to elicit a biological response (Yaffe, 2002). The initial binding event occurs at a "gatekeeper site," which, in the case of HDAC5, could be either Ser 498 or Ser 660. Taken together, these findings further substantiate the view that PKD is the principle HDAC5 kinase.

As the concept of kinase anchoring has gained acceptance, an underlying question is how AKAPs influence physiologically important phosphorylation events. One emerging theme is that aberrant signaling through AKAP complexes contributes to certain heart diseases (Diviani, 2008; McConnachie et al., 2006). For example, Yotiao anchors PKA and the phosphatase PP1 with the KCNQ1 potassium channel subunit to shape the duration of cardiac action potentials in response to β-adrenergic agonists (Chen et al., 2005; Marx et al., 2002; Westphal et al., 1999). Inherited mutations in Yotiao or the KCNQ1 channel subunit have been linked to Long QT Syndrome, a rare genetic disease characterized by stress-induced cardiac arrhythmias and sudden death (Chen et al., 2007; Kass and Moss, 2003). Likewise, the cardiac muscle-selective anchoring protein, mAKAP, assembles a cAMP signaling module consisting of PKA, PDE4D3, and Epac-1 (Dodge et al., 2001). A larger mAKAP-ryanodine receptor (RyR) complex controls excitation-contraction coupling at the sarcoplasmic reticulum (Marx et al., 2001). Pathophysiological changes in the enzyme composition of this mAKAP-RyR complex that alter the phosphorylation state of the channel have been linked to the onset of certain forms exercise induced arrhythmias in mice (Lehnart et al., 2005). We now implicate AKAP-Lbc as a cofactor that amplifies PKD signaling to HDAC5 to initiate a hypertrophic phenotype. Myocardial hypertrophy is extremely common, affecting 14%–18% of the general adult population (Benjamin and Levy, 1999; World Health Organization). Therefore, it will be important to explore the role of the AKAP-Lbc/PKD/HDAC5 signaling pathway in whole animal models to establish whether AKAP-Lbc is a valid biomarker for hypertrophic cardiomyopathy and to determine which genes are initiated upon upregulation of the anchoring protein.

EXPERIMENTAL PROCEDURES

All western blotting, RII overlays, immunoprecipitations, and phosphorylation experiments were performed as described previously (Westphal et al., 1999).

Cell Culture, Immunocytochemistry, and Live-Cell Imaging

Cos7 cells were cultured on glass coverslips. All transfections were carried out using Effectene reagent (QIAGEN, Valencia, CA). Neonatal rat cardiomyocytes were cultured as described in (Pare et al., 2005). After 1 day in culture, cells were treated with vehicle or agonist for a further 48 hrs at 37°C prior to lysis and evaluation of AKAP-Lbc expression by western blot or RT-PCR.

Preparation of primary NRVM and confocal microscopy experiments were as described in (Dodge-Kafka et al., 2005). Cells were fixed in 3.7% paraformaldehyde in PBS followed by staining for α-actinin or ANF. Secondary antibodies used were from Jackson Immunoresearch. To determine the effect of shRNA expression on cellular hypertrophy, myocytes were cotransfected with rat AKAP-Lbc shRNA-GFP or control (human AKAP-Lbc) shRNA plasmid and pEYFP (Clontech). For rescue experiments, FLAG-human AKAP-Lbc constructs were used. Anti-actinin was used to stain sarcomeric Z-disks to distinguish myocytes from contaminating fibroblasts. Images were acquired using a BioRad MRC1024 confocal microscope.

For all live-cell-imaging experiments, NRVM were cultured on glass coverslips coated with 1% gelatin (Sigma). For ectopic expression of protein, NRVM were electroporated using a modified Amaxa Nucleofector protocol. After incubation at 37°C for 18–48 hr postelectroporation, cells were washed twice with Hank's balanced salt solution, mounted in a Ludin chamber (Life Imaging Services), and imaged using a Leica AS MDW workstation. Images were acquired as described in (Dodge-Kafka et al., 2005). Cells were treated with ET-1 (100 nM working concentration) for 60 min prior to treatment with the PKC and PKD inhibitor Gö6976 (500 nM) to validate that we were measuring changes in PKD activity rather than other basophilic kinases. Nuclear phosphatase activity was inhibited by pretreatment with calyculin A (10 nM). Additional experiments were performed using cells that were pretreated with the CaMK inhibitor KN93 (5 μM working concentration for 30 min) to ensure that nDKAR was not detecting CaMK activity in NRVM.

Statistical Analyses

All data are expressed as mean ± standard error of the mean. Differences in quantitative variables were examined by one-way analysis of variance (ANOVA) or an unpaired two-tailed t test. A p value < 0.05 was considered significant (*), a p value < 0.01 was considered very significant (**), and a p value < 0.001 was considered extremely significant (***). All analyses were performed using InStat.

Experimental details for RT-PCR, expression constructs used, in vitro HDAC5 phosphorylation, 14-3-3 binding assays, and MEF2-luciferase assays are included in the Supplemental Data.

SUPPLEMENTAL DATA

The Supplemental Data include Supplemental Experimental Procedures, 11 figures, and ten movies and can be found with this article online at http://www.molecule.org/supplemental/S1097-2765(08)00681-3.

ACKNOWLEDGMENTS

This work was supported by the Fondation Leducq and the NIH (J.D.S., HL088366; A.C.N., DK54441). We thank Eric N. Olson for providing the MEF2 luciferase reporter and HDAC5-GFP constructs, Qinghong Zhang and Richard Goodman for help with luciferase assays, and Lisette Maddison and Wenbiao Chen for assistance with RT-PCR.

Received: January 25, 2008
Revised: May 7, 2008
Accepted: August 19, 2008
Published: October 23, 2008

REFERENCES

Appert-Collin, A., Cotecchia, S., Nenniger-Tosato, M., Pedrazzini, T., and Diviani, D. (2007). The A-kinase anchoring protein (AKAP)-Lbc-signaling complex mediates alpha1 adrenergic receptor-induced cardiomyocyte hypertrophy. Proc. Natl. Acad. Sci. USA *104*, 10140–10145.

Backs, J., Song, K., Bezprozvannaya, S., Chang, S., and Olson, E.N. (2006). CaM kinase II selectively signals to histone deacetylase 4 during cardiomyocyte hypertrophy. J. Clin. Invest. *116*, 1853–1864.

Bassel-Duby, R., and Olson, E.N. (2006). Signaling pathways in skeletal muscle remodeling. Annu. Rev. Biochem. *75*, 19–37.

Benjamin, E.J., and Levy, D. (1999). Why is left ventricular hypertrophy so predictive of morbidity and mortality? Am. J. Med. Sci. *317*, 168–175.

Bers, D.M., and Guo, T. (2005). Calcium signaling in cardiac ventricular myocytes. Ann. N Y Acad. Sci. *1047*, 86–98.

Black, B.L., and Olson, E.N. (1998). Transcriptional control of muscle development by myocyte enhancer factor-2 (MEF2) proteins. Annu. Rev. Cell Dev. Biol. *14*, 167–196.

Carnegie, G.K., Smith, F.D., McConnachie, G., Langeberg, L.K., and Scott, J.D. (2004). AKAP-Lbc nucleates a protein kinase D activation scaffold. Mol. Cell *15*, 889–899.

Chang, S., Bezprozvannaya, S., Li, S., and Olson, E.N. (2005). An expression screen reveals modulators of class II histone deacetylase phosphorylation. Proc. Natl. Acad. Sci. USA *102*, 8120–8125.

Chen, L., Kurokawa, J., and Kass, R.S. (2005). Phosphorylation of the A-kinase-anchoring protein Yotiao contributes to protein kinase A regulation of a heart potassium channel. J. Biol. Chem. *280*, 31347–31352.

Chen, L., Marquardt, M.L., Tester, D.J., Sampson, K.J., Ackerman, M.J., and Kass, R.S. (2007). Mutation of an A-kinase-anchoring protein causes long-QT syndrome. Proc. Natl. Acad. Sci. USA *104*, 20990–20995.

Clerk, A., and Sugden, P.H. (1999). Activation of protein kinase cascades in the heart by hypertrophic G protein-coupled receptor agonists. Am. J. Cardiol. *83*, 64H–69H.

Clerk, A., and Sugden, P.H. (2000). Small guanine nucleotide-binding proteins and myocardial hypertrophy. Circ. Res. *86*, 1019–1023.

Diviani, D. (2008). Modulation of cardiac function by A-kinase anchoring proteins. Curr. Opin. Pharmacol. *8*, 166–173. Published online December 31, 2007.

Diviani, D., Soderling, J., and Scott, J.D. (2001). AKAP-Lbc anchors protein kinase A and nucleates Galpha 12-selective Rho-mediated stress fiber formation. J. Biol. Chem. *276*, 44247–44257.

Dodge, K.L., Khouangsathiene, S., Kapiloff, M.S., Mouton, R., Hill, E.V., Houslay, M.D., Langeberg, L.K., and Scott, J.D. (2001). mAKAP assembles a protein kinase A/PDE4 phosphodiesterase cAMP signaling module. EMBO J. *20*, 1921–1930.

Dodge-Kafka, K.L., Soughayer, J., Pare, G.C., Carlisle Michel, J.J., Langeberg, L.K., Kapiloff, M.S., and Scott, J.D. (2005). The protein kinase A anchoring protein mAKAP coordinates two integrated cAMP effector pathways. Nature *437*, 574–578.

Fink, M.A., Zakhary, D.R., Mackey, J.A., Desnoyer, R.W., Apperson-Hansen, C., Damron, D.S., and Bond, M. (2001). AKAP-mediated targeting of protein kinase a regulates contractility in cardiac myocytes. Circ. Res. *88*, 291–297.

Frey, N., and Olson, E.N. (2003). Cardiac hypertrophy: the good, the bad, and the ugly. Annu. Rev. Physiol. *65*, 45–79.

Grozinger, C.M., and Schreiber, S.L. (2000). Regulation of histone deacetylase 4 and 5 and transcriptional activity by 14–3-3-dependent cellular localization. Proc. Natl. Acad. Sci. USA *97*, 7835–7840.

Kao, H.Y., Verdel, A., Tsai, C.C., Simon, C., Juguilon, H., and Khochbin, S. (2001). Mechanism for nucleocytoplasmic shuttling of histone deacetylase 7. J. Biol. Chem. *276*, 47496–47507.

Kass, R.S., and Moss, A.J. (2003). Long QT syndrome: novel insights into the mechanisms of cardiac arrhythmias. J. Clin. Invest. *112*, 810–815.

Kodama, H., Fukuda, K., Pan, J., Sano, M., Takahashi, T., Kato, T., Makino, S., Manabe, T., Murata, M., and Ogawa, S. (2000). Significance of ERK cascade compared with JAK/STAT and PI3-K pathway in gp130-mediated cardiac hypertrophy. Am. J. Physiol. Heart Circ. Physiol. *279*, H1635–H1644.

Kouzarides, T. (2007). Chromatin modifications and their function. Cell *128*, 693–705.

Kunkel, M.T., Toker, A., Tsien, R.Y., and Newton, A.C. (2007). Calcium-dependent regulation of protein kinase D revealed by a genetically encoded kinase activity reporter. J. Biol. Chem. *282*, 6733–6742.

Lehnart, S.E., Wehrens, X.H., Reiken, S., Warrier, S., Belevych, A.E., Harvey, R.D., Richter, W., Jin, S.L., Conti, M., and Marks, A.R. (2005). Phosphodiesterase 4D deficiency in the ryanodine-receptor complex promotes heart failure and arrhythmias. Cell *123*, 25–35.

Lygren, B., Carlson, C.R., Santamaria, K., Lissandron, V., McSorley, T., Litzenberg, J., Lorenz, D., Wiesner, B., Rosenthal, W., Zaccolo, M., et al. (2007). AKAP complex regulates Ca2+ re-uptake into heart sarcoplasmic reticulum. EMBO Rep. *8*, 1061–1067.

Maruyama, Y., Nishida, M., Sugimoto, Y., Tanabe, S., Turner, J.H., Kozasa, T., Wada, T., Nagao, T., and Kurose, H. (2002). Galpha(12/13) mediates alpha(1)-adrenergic receptor-induced cardiac hypertrophy. Circ. Res. *91*, 961–969.

Marx, S.O., Reiken, S., Hisamatsu, Y., Gaburjakova, M., Gaburjakova, J., Yang, Y.M., Rosemblit, N., and Marks, A.R. (2001). Phosphorylation-dependent regulation of ryanodine receptors: a novel role for leucine/isoleucine zippers. J. Cell Biol. *153*, 699–708.

Marx, S.O., Kurokawa, J., Reiken, S., Motoike, H., D'Armiento, J., Marks, A.R., and Kass, R.S. (2002). Requirement of a macromolecular signaling complex for beta adrenergic receptor modulation of the KCNQ1-KCNE1 potassium channel. Science *295*, 496–499.

McConnachie, G., Langeberg, L.K., and Scott, J.D. (2006). AKAP signaling complexes: getting to the heart of the matter. Trends Mol. Med. *12*, 317–323.

McKinsey, T.A. (2007). Derepression of pathological cardiac genes by members of the CaM kinase superfamily. Cardiovasc. Res. *73*, 667–677.

McKinsey, T.A., Zhang, C.L., and Olson, E.N. (2000). Activation of the myocyte enhancer factor-2 transcription factor by calcium/calmodulin-dependent protein kinase-stimulated binding of 14–3-3 to histone deacetylase 5. Proc. Natl. Acad. Sci. USA *97*, 14400–14405.

McKinsey, T.A., Zhang, C.L., and Olson, E.N. (2001). Identification of a signal-responsive nuclear export sequence in class II histone deacetylases. Mol. Cell. Biol. *21*, 6312–6321.

Molkentin, J.D., and Dorn, I.G., II. (2001). Cytoplasmic signaling pathways that regulate cardiac hypertrophy. Annu. Rev. Physiol. *63*, 391–426.

Mullin, M.J., Lightfoot, K., Marklund, U., and Cantrell, D.A. (2006). Differential requirement for RhoA GTPase depending on the cellular localization of protein kinase D. J. Biol. Chem. *281*, 25089–25096.

Pare, G.C., Bauman, A.L., McHenry, M., Michel, J.J., Dodge-Kafka, K.L., and Kapiloff, M.S. (2005). The mAKAP complex participates in the induction of cardiac myocyte hypertrophy by adrenergic receptor signaling. J. Cell Sci. *118*, 5637–5646.

Perrino, C., and Rockman, H.A. (2007). Reversal of cardiac remodeling by modulation of adrenergic receptors: a new frontier in heart failure. Curr. Opin. Cardiol. *22*, 443–449.

Sucharov, C.C., Langer, S., Bristow, M., and Leinwand, L. (2006). Shuttling of HDAC5 in H9C2 cells regulates YY1 function through CaMKIV/PKD and PP2A. Am. J. Physiol. Cell Physiol. *291*, C1029–C1037.

Sugden, P.H., and Clerk, A. (2005). Endothelin signalling in the cardiac myocyte and its pathophysiological relevance. Curr. Vasc. Pharmacol. *3*, 343–351.

Teerlink, J.R. (2005). Endothelins: pathophysiology and treatment implications in chronic heart failure. Curr. Heart Fail. Rep. *2*, 191–197.

van Oort, R.J., van Rooij, E., Bourajjaj, M., Schimmel, J., Jansen, M.A., van der Nagel, R., Doevendans, P.A., Schneider, M.D., van Echteld, C.J., and De Windt, L.J. (2006). MEF2 activates a genetic program promoting chamber dilation and contractile dysfunction in calcineurin-induced heart failure. Circulation *114*, 298–308.

Vega, R.B., Harrison, B.C., Meadows, E., Roberts, C.R., Papst, P.J., Olson, E.N., and McKinsey, T.A. (2004). Protein kinases C and D mediate agonist-dependent cardiac hypertrophy through nuclear export of histone deacetylase 5. Mol. Cell. Biol. *24*, 8374–8385.

Waldron, R.T., and Rozengurt, E. (2003). Protein kinase C phosphorylates protein kinase D activation loop Ser744 and Ser748 and releases autoinhibition by the pleckstrin homology domain. J. Biol. Chem. *278*, 154–163.

Westphal, R.S., Tavalin, S.J., Lin, J.W., Alto, N.M., Fraser, I.D., Langeberg, L.K., Sheng, M., and Scott, J.D. (1999). Regulation of NMDA receptors by an associated phosphatase-kinase signaling complex. Science *285*, 93–96.

Wu, X., Zhang, T., Bossuyt, J., Li, X., McKinsey, T.A., Dedman, J.R., Olson, E.N., Chen, J., Brown, J.H., and Bers, D.M. (2006). Local InsP3-dependent perinuclear Ca2+ signaling in cardiac myocyte excitation-transcription coupling. J. Clin. Invest. *116*, 675–682.

Yaffe, M.B. (2002). How do 14–3-3 proteins work?–Gatekeeper phosphorylation and the molecular anvil hypothesis. FEBS Lett. *513*, 53–57.